Arabian Journal of Geosciences (2022) 15: 878
https://doi.org/10.1007/s12517-022-10189-0

ORIGINAL PAPER

Evaluation of water retention curves in soils with different fines content

Victor Hernández[1] · **María Camila Olarte**[1] · **Juan Carlos Ruge**[1] · **Juan Gabriel Bastidas**[1] · **Camilo Ernesto Herrera**[1] · **Iván Fernando Otálvaro**[2]

Received: 13 October 2021 / Accepted: 22 April 2022 / Published online: 28 April 2022

Abstract
This research proposed to analyze the dependence on the water retention properties in granular samples (Guamo sand) regarding different contents of fines (kaolin). The extended evaporation method (EEM) and dew point method (DPM) allowed the construction of the water retention curves (WRCs). These methods can determine the matric suction of the samples at volumetric water contents in the partially saturated state. The results revealed that the Guamo sand only showed significant suction values in the pendular state of the system. As the kaolin content in the samples increased, the desaturation process revealing high suction values, even when samples have up to 30% volumetric water content. The evaluation of the experimental methods was generated from a WRC setting using traditional constitutive models. The prediction capacity of each model is defined with the coefficient of determination, where the behavior of the data indicates more significant predictive potential in high suction ranges.

Keywords Water retention curve · Extended evaporation method · Dew point method · Drying path

Introduction

The geometric simplification of the pore space to quantify physical properties and processes in unsaturated media is generally based on soil water retention capacity estimates through classical hydraulic function (Khlosi et al. 2006). The water retention curve (WRC) describes the relationship between soil capillary potential (ψ) and volumetric water content (θ_w) (Assouline et al. 1998). Although θ_w is related to microstructural porosity and degree of saturation, and ψ is linked to centimetric height, both are a single fundamental property of WRC. WRC is generally obtained from paired measurements of water content and pressure head under quasi-equilibrium conditions. However, to be helpful in descriptive processes concerning the water–air interface, the mechanical behavior of the WRC results is continuously adjusted using predictive models (Cornelis et al. 2005). In the graphical domain of WRC, the value of θ_w for a given ψ depends on the path. During the drying phase, any path is more significant than the suction in the wetting path (Likos et al., 2014). This hysteretic behavior is derived from the direct couplings between the degree of saturation, effective stresses, and matric suction.

Responsible Editor: Zeynal Abiddin Erguler

✉ María Camila Olarte
mcolarte@ucatolica.edu.co

Victor Hernández
vjhernandez@ucatolica.edu.co

Juan Carlos Ruge
jcruge@ucatolica.edu.co

Juan Gabriel Bastidas
jgbastidas@ucatolica.edu.co

Camilo Ernesto Herrera
ceherrera@ucatolica.edu.co

Iván Fernando Otálvaro
ifotalvaro@javerianacali.edu.co

[1] Programa de Ingeniería Civil, Facultad de Ingeniería, Universidad Católica de Colombia, 111311 Bogotá, Colombia

[2] Departamento de Ingeniería Civil e Industrial. Pontificia, Universidad Javeriana - Seccional Cali, 760031 Cali, Colombia

However, the suction retention capacity of a soil depends on many factors: pore size distribution, chemical condensation of the aqueous solution, particular surface activity, thixotropic effects, and particle size distribution (Aubertin et al., 2003). Knowledge of hysteresis behavior is essential for the understanding of the mechanical-hydraulic response in granular soils. A more recent emphasis is attributed to the effects of hysteresis on the functional spectrum, including deformation and shear strength (Likos and Lu 2004; Wheeler et al. 2003).

The fundamental description of the WRC establishes four saturation domains: (i) total saturation (θ_s); (ii) funicular state, defined in any matric suction range, for which the granular structure of the soil is progressively saturated in a continuous liquid–gas flow stage; (iii) pendular state, which is presented in intervals of ψ with interstitial discontinuity; and (iv) residual state (θ_r). These stages are represented in Fig. 1. The limits for each of these changes depend on the continuous nature of the flow, the number of phases, and the pore size (Vanapalli et al. 1999). Currently, the literature applied to unsaturated soil mechanics has little evidence of the accurate intrinsic contour of the WRC, since the enduring influence of the fluctuating pore mechanism on the saturation relations, and this demands a high experimental parametric calibration to determine only the retention aspects under constant porosity (Nuth and Laloui 2008).

Traditional and modern investigations exhibit variability in the WRC silhouette when different experimental techniques and wetting histories are used. Even when determined under the same scale, the bias between approaches is considerable (Cancela et al., 2006). WRC can be measured through a plurality of direct check empirical methods using technique psychometric, heat dissipation sensors, suction plates, pressure cells or columns (Campbell and Gee 2018), and many other approaches reviewed by Bittelli and Flury

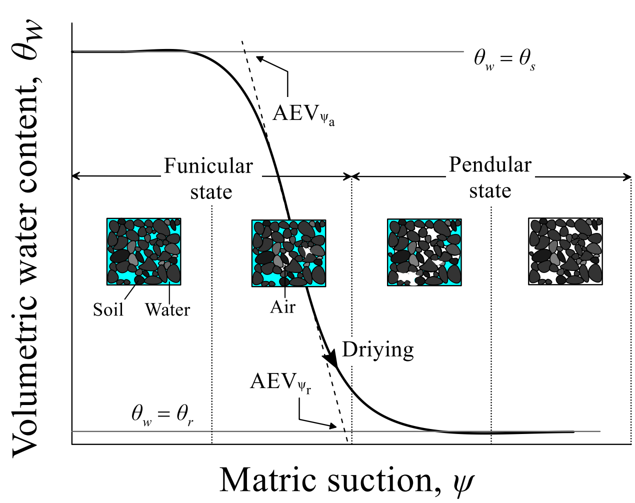

Fig. 1 Typical unimodal water retention curve

(2009). Data pairs corresponding to ψ and θw are usually analyzed in terms of analytical constitutive equations proposed (Campbell 1974; Durner 1994; Vogel and Cislerova 1998; Kosugi 1996; Fredlund and Xing 1994; Seki 2007; van Genuchten 1980) or using derivate pedotransfer functions (Acutis and Donatelli 2003; Schaap et al. 2001).

Parametric estimation in the mechanical archetypes is available, which is generally used to define WRC, involves capacity and flow attributes. It is combined with numerical solutions of the Richards equation (Richards and Reddy 2007) to obtain quantitative predictions of the hydraulic components in any given soil. Popular methods include the coupled osmotic tensiometer developed by Madsen et al. (1986) and strain infiltrometer methods (Simunek et al. 1998). However, it is possible to employ other field methods similarly. In particular, the technologies based on vapor pressure measurements are most commonly used to describe the WRC.

These approaches are derived from the pioneering studies by Gardner and Miklich (1962), where measurements of evaporation rate and tension are a direct and simultaneous quantification of the soil's water retention capacity. For such reason, the evaporation process has been interpreted analytically in the porous environment and the elemental volumetric range for multiple matric suction scales (Lehmann et al. 2008; Shokri et al. 2015; Peters et al. 2015). One of the recent versions of the evaporation technology is the HYPROP© device, whose functional principle focuses on semi-automated direct measurements of the water retention and hydraulic conductivity function for stress ranges between θ_s and θ_r, using the extended evaporation method (EEM) (Schindler et al. 2010).

There is a traced path in generating models and approaches to test the EEM system in continuous loop inflow and outflow (e.g., Bezerra-Coelho et al. 2018; Schelle et al. 2010). Schelle et al. (2013) evaluated and compared four methodologies for delimiting ψ and θ_w ranges in WRC under varying moisture scales over a wide textural range. They reported ψ intervals obtained by EEM device, comparable in the dry range with those determined from the dew point method through the WP4C instrument, although with hysteretic behaviors.

In contrast to EEM, the dew point method (DPM) system is based on the principle of equilibrium between liquid-phase water in a soil sample and vapor-phase water under closed chamber conditions (Scanlon et al. 2002). In recent research, DPM has been used extensively to determine the unmistakable silhouette of the WRC. Kirste et al. (2019) proposed to apply DPM after evaporation using pressure columns for given strain rates, testing the development of DPM to describe WRC in the humidity range, through numerical modeling. The search for accurate numerical proximities for WRC using EEM and DPM is currently researched

(Fields et al. 2020; Händel et al. 2019; Jackisch et al. 2020; Domínguez-Niño et al. 2020; Shokrana and Ghane 2020).

Materials and methods

Soils

Two types of soils were used to analyze the consistency of the EEM and DPM methods in the graphical portrait of the WRC. Sand samples from the Guamo River were selected because of their index properties commonly used in research works and kaolin as a cohesive agent to raise the stress ranges. This typology of sand presents a subangular predominance in the form according to the analyzes of digital cartography of particles using the scales of Krumbein (1941). The content of kaolin in the testing prototypes was gradually increased in the five tests, from 5 to 35% with steps of 5%, decreasing the proportion of the Guamo sand, respectively. Since for small suction values, the particle distribution affects significantly; it was necessary to use reconstituted samples for EEM and DPM, without sharp decreases in sand content. The mineral dispersion of the clay within the polymeric matrix, the physicochemical properties of the sand, and sample distribution, are summarized in Table 1.

Extended evaporation method

The EEM device (Fig. 2) was used for simplified evaporation runs. Saturated soil samples of approximately 5 cm in height and 8 cm in diameter were submitted to evaporation in the laboratory. The tensiometric matric suction was continuously monitored at depths of 2 to 4 cm. During the evaporation process, the absolute water contents were calculated by measuring the weights of the components used in the assembly, including the dry matter of the specimens with their respective configuration (Table 1—samples). According to the manufacturer, the maximum height for the air inlet of the tensiometer rings was 85 kPa. Hyprop View software was used to compute the discrete data points of the five WRC in the dry range between 0 and 3.1 pF, along with their unsaturated hydraulic conductivity in the laboratory.

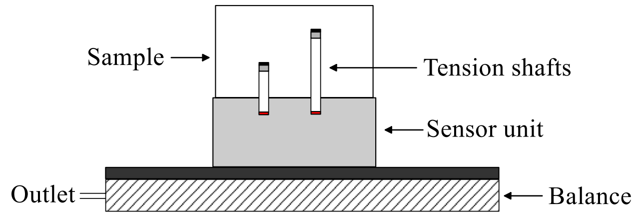

Fig. 2 Extended evaporation method devise

The matric suction was continuously monitored at depths of 2 to 4 cm.

Dew point method

For descriptive idealization of the drying range in intervals above 3.1 pF, the DPM determines the relative humidity from the sample temperature and is sufficient to generate "dew" condensation of the air by cooling, with accuracies of 1% at ψ from 4.5 to 6.5 pF. In wetter ranges (2.5–4.5 pF), the accuracy decreases, being 5% for ψ below 3.5 pF, equivalent to 500 hPa. Soil samples for each configuration were exposed to evaporation until the desired water content was reached. Six capsules were extracted from each sample configuration, two from the top, two from the bottom, and two from the middle, to construct the drying WRC. The Hyprop Fit utility software was employed for the unification of the EEM and DPM results. The two measurement methods applied and their centimeter height ranges in pF are presented in Fig. 3.

Unimodal functions

Three unimodal functions were considered to fit WRCs in this study: [1] Fredlund-Xing function (Fredlund and Xing 1994), [2] Brooks-Corey function (Brooks and Corey 1964), and [3] van Genuchten function (van Genuchten 1980). The Brooks-Corey and van Genuchten functions use porous structures to simulate flow paths in unsaturated media. On the other hand, for the Fredlund-Xing function, the interval of ψ is substantially larger than other models, providing a better description of WRC. The one-to-one relationship

Table 1 Soil properties

						Guamo Sand						Kaolin			
	Sample (%)					Physics						XRD (%)			
Soil texture	1	2	3	4	5	Gs	e_{max}	e_{min}	Cc	Cu	D_{10} (mm)	Quartz	Kaolinite	Illite	Montmorillonite
Sand	100	95	85	75	65	2.72	0.94	0.65	1.08	2.24	0.20	na	na	na	na
Clay	0	5	15	25	35	na	na	Na	na	na	0.0003	53.89	35.37	9.68	1.06

na not available

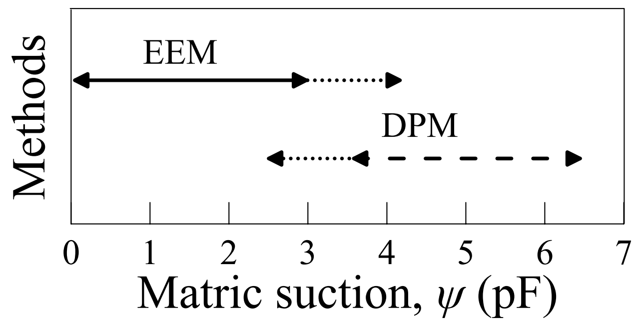

Fig. 3 Methods for determining WRC and their measurement ranges

between ψ and θ_w for each visual model is expressed as follows:

$$\theta_w = C(\psi)\frac{\theta_s}{\left\{\ln\left[e + \left(\frac{\psi}{a}\right)^n\right]\right\}^m} \tag{1}$$

$$\theta_w = \begin{cases} \theta_r + (\theta_s - \theta_r)\left(\frac{\psi}{\psi_d}\right)^{-\lambda}; \psi > \psi_d \\ \theta_s; \psi \le \psi_d \end{cases} \tag{2}$$

$$\theta_w = \theta_r + (\theta_s - \theta_r)\left[\frac{1}{1 + (\alpha\psi)^\beta}\right]^{1-\frac{1}{\beta}} \tag{3}$$

where ψ_d is the suction displacement, λ (pore distribution coefficient), and a, β, α, α, m, and n fit parameters. In the Fredlund-Xing model, e is the Napier's constant. The correction function for the variable $C(\psi)$ in terms of ψ_r analogous to θ_r, under unsaturated conditions, is represented by:

$$C(\psi) = 1 - \frac{\ln\left[1 + \left(\frac{\psi}{\psi_r}\right)\right]}{\ln\left[1 + \left(\frac{10^6}{\psi_r}\right)\right]} \tag{4}$$

Results and discussion

The weight loss by the water evaporation process is shown comparatively in Fig. 4, using the identification GS for Guamo sand, and K for kaolin. The trend of the desaturation phenomenon is independent of the material and its particular configuration. However, the higher the kaolin content in the sample, the smaller the time-space involved in completing the process. The void ratio, e, in granular soils is substantially higher than in fine size distribution, which means higher interstitial saturation. However, the gradual addition of cohesive plates reduces the e, the sample saturation, and desaturation time.

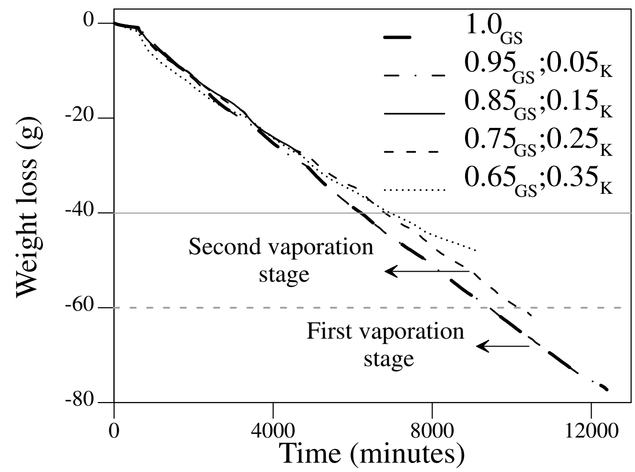

Fig. 4 Weight loss due to evaporation process

The range of the air entry point (AEV) is crucial for understanding the behavior shown in Fig. 5 since it delimits the change from the boundary effect zone to the transition effect zone and has a directly proportional relationship to the ψ. Fine soils exhibit higher ψ ranges than sands due to their laminar structure with electrochemical activity. Consequently, net stress ranges are higher for samples with higher fines content, exceeding 800 hPa.

Water retention curves

The data obtained by the EEM synthesized evaporation methodology provided information from complete saturation to approximately 3.0 pF in all samples, establishing the initial range of desaturation. The extension of the method

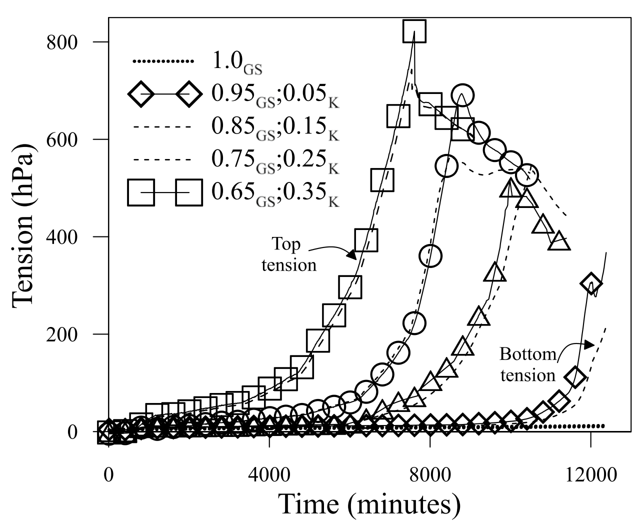

Fig. 5 *Hyprop View* predictions of the top and bottom tensions in soil samples

using DPM provided an additional dataset between 3.0 and 4.5 pF. On average, the mechanics of the results from both methods matched reasonably well for the first three samples, whose fines content is not representative. The dry scale, however, varied considerably at percentages of fines above 20%. The ψ and θ_w loops fluctuated widely in each test. For ψ values less than 4.0 pF, the DPM accuracy exceeds 5% and substantially reduces the amount of data at suction stresses above 350 hPa. This limitation of use compresses the actual expansion of the WRCs from 4.0 pF and above, with kaolin percentage above 15%.

On the other hand, EEM works quite well for determining WRC at suctions below 2.0 pF. The applicability horizon of both devices depends directly on the particle size; the higher the fines content, the higher the air entry value (AEV) is reached at higher ψ values, which translates into lower drying WRC detention at ψ above 3.0 pF. The WRCs for each specimen are given in Fig. 6.

In addition, the adequate continuity of the EEM data than the DPM data is evident, confirming the reproducibility and reliability of the extended evaporation method. The above is due to larger contact points between the sample and the upper and lower EEM plates or splicing problems of the DPM prototypes due to their size. However, a larger size for each of the samples means a longer time for the evaporation process and high degrees of data scattering. It is observed that the samples with a tendency to be completely granular (1 and 2) start with high θ_w and develop generating low

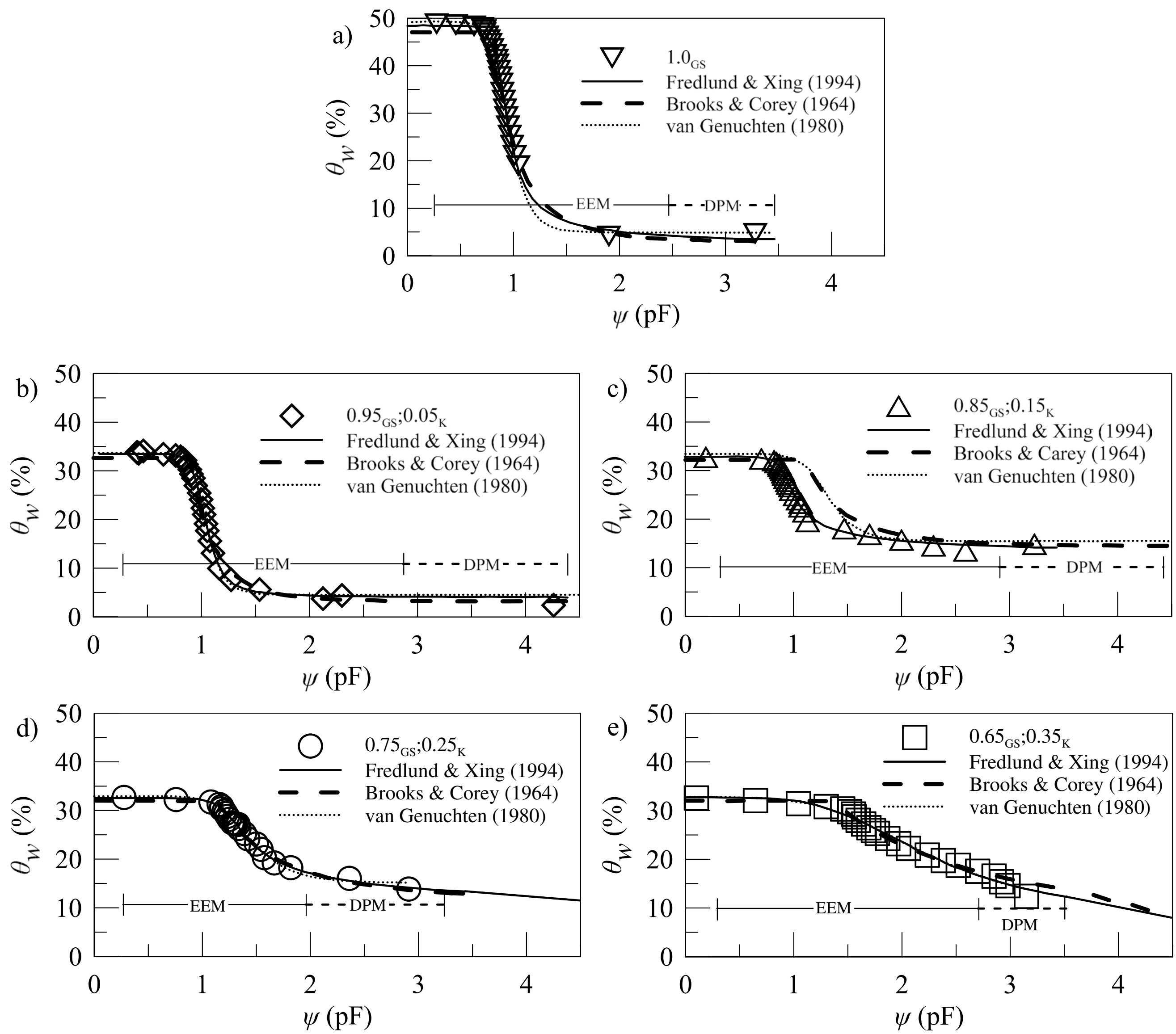

Fig. 6 Water retention curves (WRCs) obtained by EEM and DPM in **a** 100% GS, **b** 95% GS and 5% K, **c** 85% GS and 15% K, **d** 75% GS and 25% K, and **e** 65% GS and 35% K

matric suctions. For samples with high fines contents (3, 4, and 5), their θ_w start with low values, and unfold generating high matric suctions, even with considerable water contents.

Behavior of the models

The data received from the Hyprop fit were analyzed by applying a curve fitting procedure using Eqs. (1), (2), and (3). Since the objective of this research was to examine the WRC in granular soils with different fines contents, a predictive process of parametric comparison was used using only volumetric content data measured at saturation (θs) and residual (θr) as matching points, which values are reported in Table 2. For fines contents, less than 20%, the numerical variability between approaches is less than 0.8% in θs, concerning the experimentally measured values. However, the approximation is more accurate in the Fredlund-Xing model, with less than 0.3% uncertainty ranges for all samples. The van Genuchten model presents the highest variability in the residual results since its functional algorithm is prescribed for small ψ ranges and ignores the transition between porous systems.

Additionally, Table 3 shows the values of the coefficient of determination, R^2, between WRC to assess the capacity of the methods of predicting the results. Suction and volumetric water content generated R^2 values for two separate datasets. In volumetric content data, there is a better coupling of the models to the matrix of experimental results. This behavior is derivative of the dependence on low suction ranges to the distribution of particles, which leads to deviations from the data generated by the empirical method.

Regarding the Brooks-Corey model, at residual points, the singular behavior of the retention curve for ψ values lower than two pF at percentages of fines equal to 15% was not adequately described. In contrast, for samples 4 and 5, Fredlund-Xing describes near-zero θr, optimizing the intrinsic WRC convolution for ψ greater than 4.5 pF. The dispersion of the data is more noticeable in the residual mechanics than those obtained employing EEM and DPM. This singular behavior is due to the decrease in data continuity at high suctions and accuracy at θw close to θr. However, the choice of the most appropriate equation for application purposes depends on the objective of the analysis. A more detailed description of the WRC using more simplified numerical representations with better-identified parameters may be preferable or vice versa.

Table 3 Coefficient of determination R^2 for ψ and θ_w between models and experimental data

Model	Experimental data	
	ψ	θ_w
Fredlund and Xing (1994)	0.74	0.93
Brooks and Corey (1964)	0.69	0.92
van Genuchten (1980)	0.72	0.78

Conclusions

A directly proportional relationship can be established from the WRC obtained between the content of fines in a soil sample and suction, even at high volumetric water contents. Therefore, these data reflected in WRC under the framework of partially saturated soil mechanics are fundamental for analyzing the hydraulic characterization of soils and the behavior of the interstitial flow.

For the soils in question, the higher the fines content, the WRC description develops over a wider range of matric suction, since in particular cohesive configurations, the suction stress is substantially increased to mostly granular soils. The extended vaporization method estimates more accurately, in all cases, the WRC and its parameters, at least in the ψ range used in the current analysis. However, it is advisable to extend its applicability with DPM if fine soils are used since the suction stress range is raised, and data continuity is required at ψ higher than those defined by EEM.

Table 2 Water retention curve parameters for soils under study using unimodal functions

	Experimental		Fredlund and Xing (1994)		Brooks and Corey (1964)		van Genuchten (1980)	
Sample	θ_s (%)	θ_r (%)	θ_s (%)	θ_r (%)	θ_s (%)	θ_r (%)	θ_s (%)	θ_r (/%)
1	48.79	4.65	48.39	0.89	46.99	2.66	49.18	4.85
2	34.08	2.38	33.56	4.00	32.64	3.08	33.66	4.57
3	32.77	14.85	32.75	9.50	32.15	14.27	33.36	15.47
4	32.68	10.72	32.54	1.5e − 4	32.03	11.02	33.02	14.97
5	32.59	11.74	32.64	4.9e − 5	32.05	1.2e − 5	32.74	8.00

θ_s volumetric water content in saturation, θ_r residual volumetric water content

Declarations

Conflict of interest The authors declare no competing interests.

References

Acutis M, Donatelli M (2003) SOILPAR 2.00: software to estimate soil hydrological parameters and functions. Eur J Agron 18(3–4):373–7. https://doi.org/10.1016/S1161-0301(02)00128-4

Assouline S, Tessier D, Bruand A (1998) A conceptual model of the soil water retention curve. Water Resour Res 34(2):223–231. https://doi.org/10.1029/97WR03039

Aubertin M, Mbonimpa M, Bussière B, Chapuis RP (2003) A model to predict the water retention curve from basic geotechnical properties. Can Geotech J 40(6):1104–1122. https://doi.org/10.1139/t03-054

Bezerra-Coelho CR, Zhuang L, Barbosa MC, Soto MA, Van Genuchten MT (2018) Further tests of the HYPROP evaporation method for estimating the unsaturated soil hydraulic properties. J Hydrol Hydromech 66(2):161–169. https://doi.org/10.1515/johh-2017-0046

Bittelli M, Flury M (2009) Errors in water retention curves determined with pressure plates. Soil Sci Soc Am J 73(5):1453–1460. https://doi.org/10.2136/sssaj2008.0082

Brooks RH, Corey AT (1964) Hydraulic properties of porous media. Colorado State University, Libraries

Campbell G (1974) A simple method for determining unsaturated conductivity from moisture retention data. Soil Sci 117(6):311–314

Campbell GS, Gee GW (2018) Water potential: miscellaneous methods. Methods of Soil Analysis: Part 1 Physical and Mineralogical Methods, vol 5. pp. 619–33. https://doi.org/10.2136/sssabookser5.1.2ed.c25.

Cancela JJ, Dafonte J, Martínez EM, Cuesta TS, Neira XX (2006) Assessment of a water activity meter for rapid measurements of soil water potential. Biosyst Eng 94(2):285–295. https://doi.org/10.1016/j.biosystemseng.2006.02.018

Cornelis WM, Khlosi M, Hartmann R, Van Meirvenne M, De Vos B (2005) Comparison of unimodal analytical expressions for the soil-water retention curve. Soil Sci Soc Am J 69(6):1902–1911. https://doi.org/10.2136/sssaj2004.0238

Domínguez-Niño JM, Arbat G, Raij-Hoffman I, Kisekka I, Girona J, Casadesús J (2020) Parameterization of soil hydraulic parameters for HYDRUS-3D simulation of soil water dynamics in a drip-irrigated orchard. Water 12(7):1858. https://doi.org/10.3390/w12071858

Durner W (1994) Hydraulic conductivity estimation for soils with heterogeneous pore structure. Water Resour Res 30(2):211–223. https://doi.org/10.1029/93WR02676

Fields JS, Owen JS, Stewart RD, Heitman JL, Caron J (2020) Modeling water fluxes through containerized soilless substrates using HYDRUS. Vadose Zo J 19(1). https://doi.org/10.1002/vzj2.20031.

Fredlund DG, Xing A (1994) Equations for the soil-water characteristic curve. Can Geotech J 31(4):521–532. https://doi.org/10.1139/t94-061

Gardner WR, Miklich FJ (1962) Unsaturated conductivity and diffusivity measurements by a constant flux method. Soil Sci 93(4):271–274

Händel F, Fichtner T, Graeber P-W (2019) Numerical and laboratory investigations of closely-spaced and joint infiltration of precipitation and treated waste water. Water 11(11):2262. https://doi.org/10.3390/w11112262

Jackisch C, Germer K, Graeff T, Andrä I, Schulz K, Schiedung M et al (2020) Soil moisture and matric potential-an open field comparison of sensor systems. Earth Syst Sci Data 12(1):683–697

Khlosi M, Cornelis WM, Gabriels D, Sin G (2006) Simple modification to describe the soil water retention curve between saturation and oven dryness. Water Resour Res 42(11). https://doi.org/10.1029/2005WR004699.

Kirste B, Iden SC, Durner W (2019) Determination of the soil water retention curve around the wilting point: optimized protocol for the dewpoint method. Soil Sci Soc Am J 83(2):288–299. https://doi.org/10.2136/sssaj2018.08.0286

Kosugi K (1996) Lognormal distribution model for unsaturated soil hydraulic properties. Water Resour Res 32(9):2697–2703. https://doi.org/10.1029/96WR01776

Krumbein WC (1941) Measurement and geo-logical significance of shape and roundness of sedimentary particles. J Sediment Res 11(2):64–72

Lehmann P, Assouline S, Or D (2008) Characteristic lengths affecting evaporative drying of porous media. Phys Rev E 77(5):056309. https://doi.org/10.1103/physreve.77.056309

Likos WJ, Lu N (2004) Hysteresis of capillary stress in unsaturated granular soil. J Eng Mech 130(6):646–655. https://doi.org/10.1061/(ASCE)0733-9399(2004)130:6(646)

Likos WJ, Lu N, Godt JW (2014) Hysteresis and uncertainty in soil water-retention curve parameters. J Geotech Geoenvironmental Eng 140(4):04013050. https://doi.org/10.1061/(ASCE)GT.1943-5606.0001071

Madsen HB, Jensen CR, Boysen T (1986) A comparison of the thermocouple psychrometer and the pressure plate methods for determination of soil water characteristic curves. J Soil Sci 37(3):357–362. https://doi.org/10.1111/j.1365-2389.1986.tb00368.x

Nuth M, Laloui L (2008) Advances in modelling hysteretic water retention curve in deformable soils. Comput Geotech Elsevier 35(6):835–844. https://doi.org/10.1016/j.compgeo.2008.08.001

Peters A, Iden SC, Durner W (2015) Revisiting the simplified evaporation method: identification of hydraulic functions considering vapor, film and corner flow. J Hydrol 527:531–542. https://doi.org/10.1016/j.jhydrol.2015.05.020

Richards KS, Reddy KR (2007) Critical appraisal of piping phenomena in earth dams. Springer 66(4):381–402. https://doi.org/10.1007/s10064-007-0095-0

Scanlon BR, Andraski BJ, Bilskie J (2002) 3.2.4 Miscellaneous methods for measuring matric or water potential. Methods Soil Anal Part 4 Phys Methods 5:643–70. https://doi.org/10.2136/sssabookser5.4.c23

Schaap MG, Leij FJ, Van Genuchten MT, Brown GE (2001) Rosetta: a computer program for estimating soil hydraulic parameters with hierarchical pedotransfer functions. Elsevier 251(3–4):163–176. https://doi.org/10.1016/S0022-1694(01)00466-8

Schelle H, Iden SC, Peters A, Durner W (2010) Analysis of the agreement of soil hydraulic properties obtained from multistep-outflow and evaporation methods. Vadose Zo J 9(4):1080–1091. https://doi.org/10.2136/vzj2010.0050

Schelle H, Heise L, Jänicke K, Durner W (2013) Water retention characteristics of soils over the whole moisture range: a comparison of laboratory methods. Eur J Soil Sci 64(6):814–821. https://doi.org/10.1111/ejss.12108

Schindler U, Durner W, von Unold G, Müller L (2010) Evaporation methodfor measuring unsaturated hydraulic properties of soils: Extending the measurement range. Soil science society of America journal 74(4):1071–1083. https://doi.org/10.2136/sssaj2008.0358

Seki K (2007) Fitting of soil water retention SWRC fit-a nonlinear fitting program with a water retention curve for soils having unimodal and bimodal pore structure. Hydrol Earth Syst Sci Discuss 4(1):407–437. https://doi.org/10.5194/hessd-4-407-2007

Shokrana MSB, Ghane E (2020) Measurement of soil water characteristic curve using HYPROP2. MethodsX 7:100840. https://doi.org/10.1016/j.mex.2020.100840

Shokri N, Or D, Weisbrod N, Prat M (2015) Drying of porous media. Transp Porous Media 110(2):171–3. https://doi.org/10.1007/s11242-015-0577-7

Simunek J, Wang D, Shouse PJ, Van Genuchten MT (1998) Analysis of field tension infiltrometer data by parameter estimation. Int Agrophys 12(3)

van Genuchten MT (1980) A closed-form equation for predicting the hydraulic conductivity of unsaturated soils. Soil Sci Soc Am J 44(5):892–898. https://doi.org/10.2136/sssaj1980.03615995004400050002x

Vanapalli SK, Fredlund DG, Pufahl DE (1999) The influence of soil structure and stress history on the soil-water characteristics of a compacted till. Geotechnique 49(2):143–159

Vogel T, Cislerova M (1998) On the reliability of unsaturated hydraulic conductivity calculated from the moisture retention curve. Transp Porous Media 3(1):1–15. https://doi.org/10.1007/bf00222683

Wheeler SJ, Sharma RS, Buisson MSR (2003) Coupling of hydraulic hysteresis and stress-strain behaviour in unsaturated soils. Geotechnique 53(1):41–54. https://doi.org/10.1680/geot.2003.53.1.41